Eurasian Chem.-Technol. J. 28 (2026) 181–188
The journal of the Institute of Combustion Problems https://ect-journal.kz

https://doi.org/10.18321/ectj1693

Investigation of the Chemical Interactions in the Na_2MoO_4-Glycerol-$ZrOCl_2$-$ErCl_3$-H_2O System and Luminescent Characteristics of the Resulting Solid Precipitate

Lusik Gegham Nersisyan* and Hayk Razmik Petrosyan

Yerevan State University, 1, A. Manoogian Str., 0025 Yerevan, Armenia

Article info

Received:
19 March 2026

Received in revised form:
4 May 2026

Accepted:
16 June 2026

Keywords:
Rare-earth elements
Glycerol
Luminescent
Hydrocomposite
Lanthanide

Abstract

The paper presents the synthesis of a solid hydrocomposite material in a water-glycerol medium based on $[MoO_4]^{2-}$, Zr^{4+}, Er^{3+}, and Na ions in a 1:1:1:3 molar ratio using directional mixing of solutions in a U-shaped vessel. X-ray diffraction analysis confirmed the partially amorphous structure of the synthesized product. Infrared spectroscopy revealed the presence of bound water molecules and characteristic functional groups, including hydroxyl, aliphatic, and metal-hydroxide fragments, as well as bands characteristic of $[MoO_4]^{2-}$ ions. Elemental and atomic emission analyses confirmed the presence of all the initial ions and revealed the molar ratio of the elements. X-ray microanalysis demonstrated chemical heterogeneity of the solid phase, while electron microscopy revealed an overall morphological homogeneity of the particles. Investigation of the luminescent properties showed the superposition of several peaks in the visible spectrum associated with transitions in the 4f shell of erbium ions, indicating the material's potential for applications in biomedicine, sensors, and optoelectronics. Thermal analysis further confirmed the presence of chemically bonded water molecules. The obtained results provide a basis for further investigation and targeted modification of the properties of such hydrocomposite systems.

1. Introduction

The relevance of this research is driven by the growing importance of rare earth elements (REEs), zirconium compounds, and molybdate-based materials in medicine and various industrial fields [1–4]. The luminescent properties of lanthanide-based compounds are comparable to those of noble metal complexes currently in use; however, lanthanide compounds offer a significant advantage in terms of lower production costs [5–7]. Luminescent materials are capable of emitting visible light upon external excitation [8, 9]. Their applications are extremely diverse and include security marking technologies, light-emitting devices, optoelectronic components, and, in particular, organic light-emitting diodes (OLEDs), which are widely utilized in modern photonic and display technologies, as well as in laser systems [10–12].

Previously, organometallic compounds of noble metals (primarily platinum and palladium) were used in industry [13]. However, such compounds have several drawbacks: their synthesis is complex and expensive, and the emission itself is characterized by low monochromaticity [14]. In contrast, coordination compounds of lanthanides are highly monochromatic and significantly less expensive, making them particularly attractive for the creation of Red, Green, Blue (RGB) lasers and selective optical materials [15, 16].

Recently, considerable attention has been devoted to the development of multifunctional optical materials. Such materials are expected to simultaneously possess several important properties, including reduced optical loss over a wide spectral range,

*Corresponding author.
E-mail address: nersisyanlusik@mail.ru

specific refractive indices, high photoluminescence intensity, increased photosensitivity, and stable and bright emission due to Raman scattering [17–21].

The combination of these properties is particularly important for the development of compact planar waveguides, optical amplifiers, lasers, frequency converters, and electrolytic modulators [22].

Rare-earth compounds containing two cations are capable of efficiently emitting red light when exposed to ultraviolet light. Even low concentrations of these compounds can provide high luminescence brightness [23].

Erbium (Er^{3+}) plays a significant role in coordination chemistry owing to its distinctive photophysical properties. Erbium-doped materials have attracted considerable attention due to their characteristic near-infrared emission at approximately 1.54 μm, which coincides with the low-loss transmission window of optical fiber communication systems, making them highly relevant for optical telecommunications. While inorganic Er^{3+}-doped materials typically exhibit relatively narrow emission bands, organic erbium complexes often display broader luminescence spectra and enhanced solubility in organic matrices [24]. In addition, these complexes enable efficient energy transfer processes through sensitizing ligands, which absorb excitation energy and subsequently transfer it to the Er^{3+} ion. This combination of strong luminescence, tunable optical properties, and compatibility with organic systems renders erbium-based coordination compounds particularly promising for applications in photonic and optoelectronic devices [25].

Less well known but no less interesting in the field of coordination chemistry, glycerol turns out to be a suitable ligand, capable of binding to one or more metal centers either directly in its triol form H_3gly (a rather rare phenomenon) or in various deprotonated glycerolate forms such as $[H_2gly]^-$, $[Hgly]^{2-}$, and $[gly]^{3-}$ (in most cases) [26]. Since the 1970s, various molecular structures obtained from glycerol and metal and organometallic precursors have been isolated and characterized, ranging from mononuclear complexes to complex aggregates and coordination polymers. Based on the single crystal X-ray diffraction structures reported so far in the literature and deposited in the Cambridge Structural Database, this structural review examines the different modes of coordination of glycerol and glycerolates with metals [27].

In the present work, compounds containing molybdenum, zirconium, and rare earth elements (Er) in an aqueous glycerol medium. In these materials, the REE activator is incorporated into inorganic frameworks, forming amorphous powdered substances with pronounced luminescent properties. Previous studies have been carried out in purely aqueous media; however, in the present work, a water–glycerol system is investigated, taking into account literature reports indicating a high probability of diffusion-controlled crystallization in such mixed solvents [28].

2. Experimental part

The following reagents were used as starting materials: glycerol (≥99%, Sigma-Aldrich, USA), $Na_2MoO_4 \cdot 2H_2O$ (≥99.5%, Merck, Germany), $ZrOCl_2 \cdot 8H_2O$ (98%, Merck, Germany), and $ErCl_3 \cdot 6H_2O$ (99.995%, Merck, Germany). The synthesis procedure was carried out as follows. Equal volumes of glycerol and water (8 mL each) were introduced into a U-shaped vessel. Subsequently, 6 mL of a 0.0018 mol sodium molybdate (Na_2MoO_4) solution were slowly added from the right side of the vessel. Thereafter, 6 mL of a 0.0018 mol erbium chloride ($ErCl_3$) solution and 6 mL of a 0.0018 mol zirconium oxychloride ($ZrOCl_2$) solution were sequentially and gradually introduced from the left side. The molar ratio of 1:1:1:3 was selected in accordance with our previous studies [29, 30].

The Mo^{6+} concentration was determined by complexometric titration, while Er^{3+} and Zr^{4+} concentrations were determined gravimetrically by precipitation of hydroxide groups with ammonia. It should be noted that when adding salts to a glycerol-water solution, a precipitate (cotton-like) immediately formed; the vessel was then tightly sealed on both sides to prevent carbonation. Over the course of 15 days of daily observation, it was noted that the contents of the vessel slowly acquired a slightly blue color on the right side, and a slightly pink color on the left side. Then, over the course of 45–50 days, a chemical reaction resulted in the formation of a homogeneous dark blue substance that did not dissolve during filtration; the volume of the precipitate no longer changed, and the pH of the filtrate was 3.5. This spatial color evolution may be related to diffusion processes accompanying metal-ligand complex formation and the development of concentration gradients within the reaction medium. The solid phase was separated from the filtrate, washed several times with deionized water, and dried in an oven at 50–60 °C. The filtrate after precipitation was not subjected to full quantitative analysis; therefore, residual metal concentrations in solution were not directly determined. The present study focused on the composition of the isolated solid phase.

IR spectra were recorded using a Perkin Elmer Spectrum 65 Fourier-transform infrared (FTIR) spectrometer (Perkin Elmer Inc., USA) equipped with an attenuated total reflectance (ATR) in the spectral range of 400–4000 cm^{-1}.

The composition of the solid phase was determined by qualitative and quantitative elemental analysis using inductively coupled plasma atomic emission spectroscopy (iCAP PRO XP, Thermo Scientific, USA). The homogeneity and elemental composition of the samples were investigated by scanning electron microscopy (SEM) using a Carl Zeiss EVO-10 microscope (Carl Zeiss AG, Germany) coupled with energy dispersive X-ray analysis (EDX).

Carbon and hydrogen contents were determined using a EuroVector EA3000 CHNS elemental analyzer (EuroVector S.p.A., Italy).

The luminescent properties of the synthesized material were investigated by fluorescence spectroscopy using a PerkinElmer LS 55 single-beam spectrometer (PerkinElmer Inc., USA). Measurements were performed under the following conditions: a 150 W pulsed xenon lamp (50 Hz) was used as the excitation source, and a Monk-Gillieson monochromator was employed over the spectral range of 200–700 nm. The spectral slit widths were set to 10 nm for both excitation and emission, and the scanning speed was 600 nm/min. A solid-sample accessory was used for measurements. Approximately 1 mg of the sample was placed in a dedicated 10 mm diameter solid-state cuvette and inserted into the instrument for recording emission and excitation spectra. Excitation wavelengths were selected based on the electronic absorption spectrum of the sample. The resulting luminescence spectrum is broad and exhibits main emission maxima at 420, 485, and 532 nm.

Thermal analysis combining thermogravimetric analysis (TGA) and differential thermal analysis (DTA) was carried out using a DTG-60 synchronous thermal analyzer (Shimadzu, Japan) under argon flow of 100 ml/min at a heating rate of 10 °C/min in the temperature range of 23–400 °C. The study was conducted in an aluminum crucible under a lid with a hole. The sample mass was 6.69 mg.

3. Results and Discussions

The resulting precipitate was separated from the filtrate, thoroughly washed with deionized water, and dried in an oven at 60 °C. The results of IR spectroscopic analysis of the resulting solid phase sample are shown in Fig. 1.

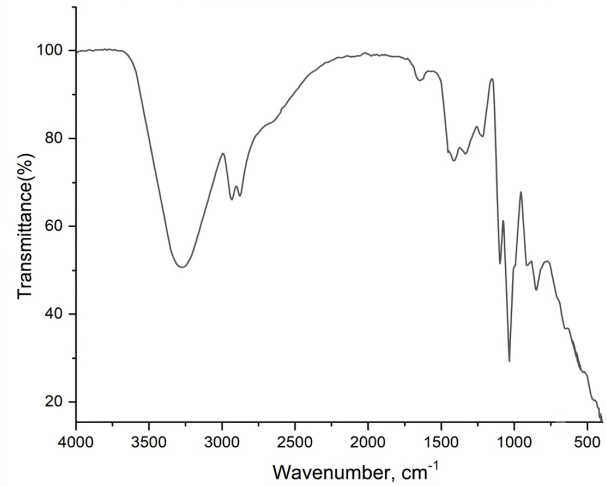

Fig. 1. IR spectrum of the obtained solid precipitate.

Absorption bands are observed at υ3273 cm^{-1} (characteristic of the stretching vibrations of associated hydroxyl groups υH-OH) and at 1648 cm^{-1} and 1565 cm^{-1}, corresponding to the deformation vibrations of δH_2O.

Analysis of the spectrum indicates that some water molecules are incorporated into the structure of the synthesized substance and are not surface-adsorbed. The spectrum also contains absorption bands at 2938 cm^{-1} and 2880 cm^{-1}, corresponding to aliphatic stretching vibrations of C-H. A weakened peak associated with hydrogen bonds is observed at 2648 cm^{-1}.

Absorption bands at 1459 cm^{-1}, 1417 cm^{-1}, 1341 cm^{-1}, and 1222 cm^{-1} correspond to deformation vibrations of OH groups (δOH). Stretching vibrations of C-O groups are observed in the region of 1100 and 1035 cm^{-1}. Stretching vibrations of υ(O-H) are detected at 653 cm^{-1}, and absorption bands in the range of 450 and 402 cm^{-1} may correspond to O-Me bonds where Me predominantly refers to Zr and/or Er centers, since Mo is present mainly as MoO_4^{2-}oxyanions rather than participating in metal-oxygen lattice vibrations. However, an unambiguous assignment of these bands specifically to Zr or Er requires more detailed and advanced structural investigations.

The absorption band at 994.63 cm^{-1} can be attributed to deformation vibrations of metal hydroxide fragments, characteristic of hydrocomposites (hydrocomplexes) [31].

The IR spectrum clearly shows absorption bands corresponding to internal vibrations of the $[MoO_4]^{2-}$ group. The bands at 851 cm^{-1} and 817 cm^{-1} are associated with degenerate vibrations $\upsilon_3(F)$. The absorption band at 708 cm^{-1} corresponds to the triply degenerate antisymmetric stretching vibration $\upsilon(F_2)$ (υ_{as}) $[MoO_4]^{2-}$.

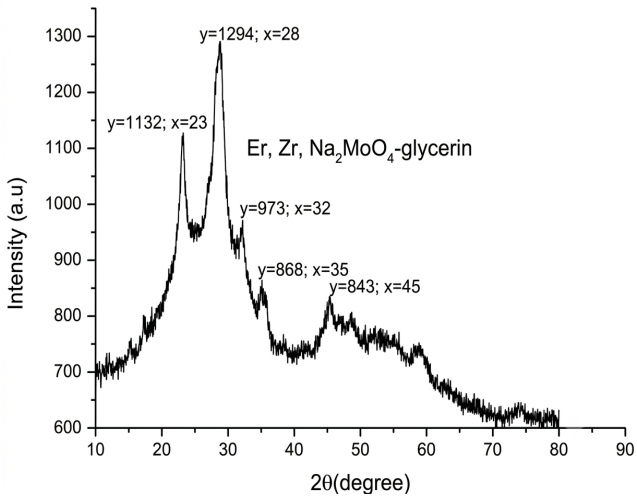

Fig. 2. X-ray pattern of the obtained solid precipitate.

X-ray diffraction analysis (Fig. 2) reveals that the synthesized sample possesses a partially amorphous structure. The diffraction pattern differs significantly from those of the starting components and cannot be described as a simple superposition of known crystalline phases, suggesting the formation of a new solid-state organization within the system. The observed broadened and weak reflections prevent reliable peak indexing and lattice parameter determination, making definitive structural identification based solely on XRD impossible. Therefore, additional advanced structural investigations are required to elucidate the structure of the synthesized material.

According to thermal analysis results (Fig. 3), the sample begins to lose mass at 40 °C, likely due to the release of water adsorbed on the sample surface (Δm = 0.45%). In the temperature range of 60–119 °C, the release of chemically bound water molecules occurs, accompanied by an endothermic peak on the DTA curve with a maximum at 91 °C and a mass loss of Δm = 2.33%.

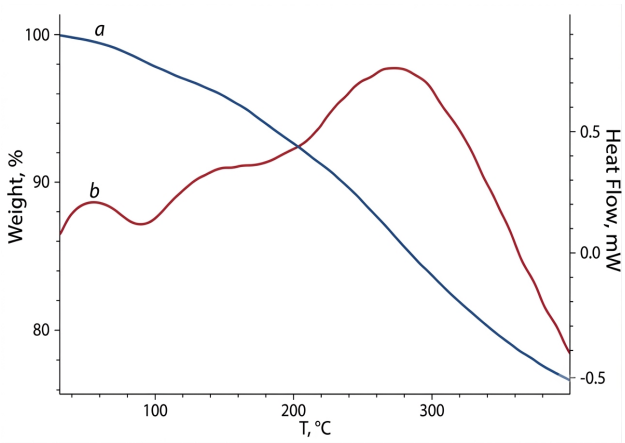

Fig. 3. TGA (a) and DTA (b) curves for the sample.

Further heating to 400 °C results in a gradual mass loss according to DTG (Δm = 20.64%) and is accompanied by a weak, complex-shaped exothermic effect on the DTA curve with an extremum at 272 °C. The total mass loss of the sample in the studied temperature range is 23.42%. It is known from the literature that pure glycerol completely evaporates in an inert nitrogen atmosphere in the range of 125–255 °C [32]. The increase in the glycerol elimination temperature in the sample is likely due to its coordination by metal centers. Such a pronounced shift in decomposition temperature is characteristic of ligand-metal interactions and indicates that glycerol acts as a coordinating ligand bound to Er^{3+} and Zr^{4+} centers rather than being present as a free or physically adsorbed molecule.

Based on the results of IR spectroscopy and thermal analysis, which revealed the presence of chemically bound water, as well as hydroxyl (aliphatic) and metal-hydroxyl functional groups, it can be concluded that the synthesized substance is a hydroxo-composite material. The quantitative composition of the partially amorphous solid phase, determined by atomic emission spectrometry, as well as the elemental analysis of the substance for carbon content, are presented in Tables 1–2. It should be noted that the study did not include a full mass balance of the system; therefore, distribution of metal ions between solid and liquid phases was not quantified.

Table 1. Quantitative results of inductively coupled plasma atomic emission spectroscopy (ICP AES)

Element	Mass fraction, %
Er	2.42
Na	0.58
Zr	11.35
Mo	12.43

The partially amorphous sample contains all the ions corresponding to the original components, but quantitative results indicate chemical heterogeneity of the composition. The molar ratio of the elements included in the solid phase can be represented as follows: nNa : nMo : nEr : nZr : nC : nH : nO = 0.025 : 0.129 : 0.0145 : 0.125 : 1.626 : 4.71 : 3.063 x 0.233 H_2O.

Table 2. Results of quantitative elemental analysis of the substance for carbon and hydrogen content

Element	Mass fraction, %
C	19.51
H	4.71

It should be noted that the quantitative composition of the solid phase, determined by atomic emission spectrometry, as well as the elemental analysis of the substance for carbon content, are given as the average result of four parallel determinations.

The scanning electron images of the powder sample in Fig. 4 suggest that the substance as a whole consists of particles of a single morphological type. However, the X-ray microanalysis results in Fig. 5 confirm that the material is structurally heterogeneous. Quantitative X-ray microanalysis data are presented in Table 3.

Table 3. Percentage ratio of elements and assessment of homogeneity of the solid phase composition

Element	Weight %	Atomic %
C	20.24	34.84
O	44.16	57.06
Na	0.70	0.63
Zr	15.85	3.59
Mo	16.62	3.58
Er	2.44	0.30

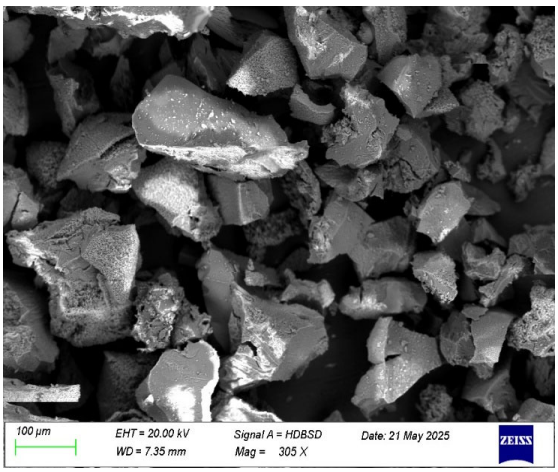

Fig. 4. SEM image of the obtained solid sediment.

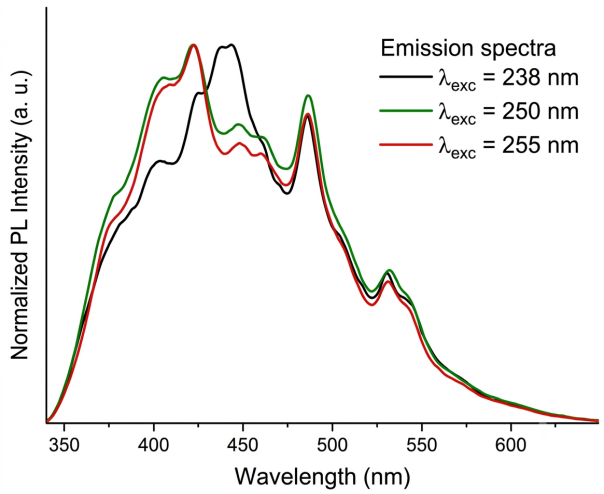

Fig. 6. Luminescence spectra of the sample.

The luminescent properties of the synthesized sample were investigated, and the corresponding emission spectra are presented in Fig. 6. The spectra are characterized by a superposition of several maxima in the visible spectral range from 350 to 600 nm. In the case of erbium, luminescence occurs due to transitions between different levels in the 4f shell. These transitions can overlap, creating a complex spectrum with several maxima in this range.

The emission spectra consist of several broad and partially overlapping bands in the 350–600 nm region. Although the broad character of the spectra prevents unambiguous assignment of each individual maximum, the observed blue-green emissions are consistent with electronic transitions involving excited 4f states of Er^{3+} ions [33]. Similar luminescence behavior has been reported for erbium-containing inorganic and coordination materials, where the emission originates predominantly from intra-4f transitions weakly influenced by the surrounding ligand field [34]. The broadening observed in the present system may additionally reflect structural disorder and the partially amorphous nature of the synthesized material [35].

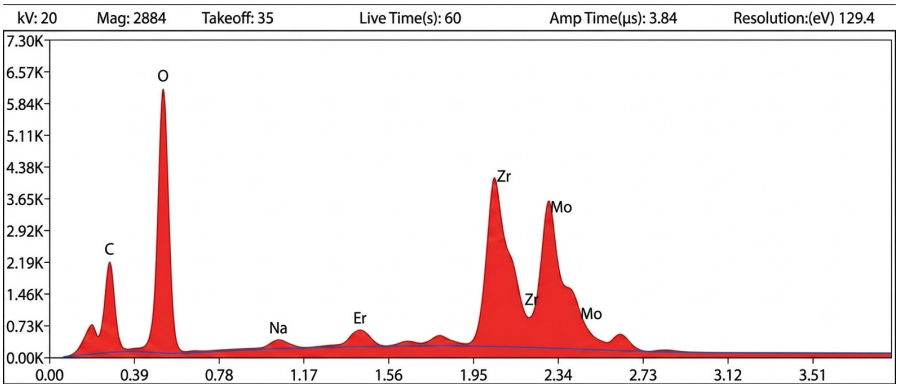

Fig. 5. X-ray microanalysis spectra of the obtained solid precipitate.

This behavior is typical of rare-earth ions, as their electron transitions in the 4f shell are weakly dependent on the crystal field, leading to narrow and separated luminescence bands. Erbium's green emission can be used as a biomarker for fluorescence imaging of cells and tissues, in the treatment of cancer cells using photodynamic therapy, in optoelectronic devices, lasers, and for the creation of temperature sensors and detectors.

4. Conclusion

The study demonstrated the formation of a partially amorphous solid hydrocomposite material containing Mo, Zr, Er, Na, glycerol-derived fragments, and bound water molecules.

The combined results of physicochemical studies confirmed the preservation of molybdate structural fragments, the presence of organic components, and the participation of glycerol in the formation of the coordination environment of the metal centers.

It was established that the synthesized system is characterized by a complex non-stoichiometric composition and chemical heterogeneity, likely due to the different affinities of the components for oxygen-containing ligands, as well as the formation of intermediate coordination forms during the synthesis process. The obtained data also indicate the interaction of glycerol with the metal centers and its involvement in the material structure not only as a solvent but also as a coordinating component.

Luminescence studies revealed the presence of characteristic emission associated with the electron transitions of Er^{3+} ions, confirming the retention of their optical activity within the hydrocomposite. This circumstance makes such systems promising for further study in terms of developing functional materials with tailored optical properties.

Since the quantitative distribution of metal ions between the solid and liquid phases was not determined in this study, the system under consideration should be interpreted as an open system in which diffusion processes and selective incorporation of components into the solid phase can play a significant role.

Overall, the obtained results demonstrate the effectiveness of the proposed approach to the synthesis of multicomponent luminescent hydrocomposite materials and provide a basis for further research into their structure, formation mechanisms, and potential applications in biomedicine, chemical analysis, and optoelectronics.

Acknowledgments

This work was supported by the Higher Education and Science Committee MESCS RA [Research project № 25YR-1D022].

This work was supported by the Higher Education and Science Committee of RA (Research project №25PTS-1D013).

References

[1]. B. Zhou, Z. Li, C. Chen, Global Potential of Rare Earth Resources and Rare Earth Demand from Clean Technologies, *Minerals* 7 (2017) 203. DOI: 10.3390/min7110203

[2]. M.M. Pylypenko, A.O. Drobyshevska, R.V. Azhazha, I.G. Tantsyura, V.M. Pelykh, Zirconium materials for medical applications, *Probl. At. Sci. Technol.* 1 (2024) 59–63. DOI: 10.46813/2024-149-059

[3]. R. Karthik, B. Mutharani, S.-M. Chen, J. Vinoth Kumar, M. Abinaya, et al., Synthesis, characterization and catalytic performance of nanostructured dysprosium molybdate catalyst for selective biomolecule detection in biological and pharmaceutical samples, *J. Mater. Chem. B* 7 (2019) 5065–5077. DOI: 10.1039/C9TB01020C

[4]. H. Petrosyan, M. Mnatsakanyan, I. Karapetyan, A. Manukyan, G. Elbakyan, et al., Establishing 18F-PSMA-1007 Production in Armenia: Radiosynthesis and Comprehensive Quality Control, *Iran J. Pharm. Res.* 25 (2026) e169428. DOI: 10.5812/ijpr-169428

[5]. T. Suemoto, S. Ono, A. Asahara, T. Okuno, T. Suzuki, et al., Comprehensive Study on the Luminescence Properties of Elemental Metals, *Phys. Rev. B* 111 (2025) 035150. DOI: 10.1103/PhysRevB.111.035150

[6]. C.M. Aikens, Electronic and Geometric Structure, Optical Properties, and Excited State Behavior in Atomically Precise Thiolate-Stabilized Noble Metal Nanoclusters, *Acc. Chem. Res.* 51 (2018) 3065–3073. DOI: 10.1021/acs.accounts.8b00364

[7]. V.A. Lapina, T.A. Pavich, A.V. Trofimov, N.N. Trofimova, Yu.B. Tsaplev, Luminescent materials for modern light sources, *Russ. Chem. Rev.* 86 (2017) 831–844. DOI: 10.1070/RCR4735

[8]. X. Li, Y. Xie, Z. Li, Diversity of Luminescent Metal Complexes in OLEDs: Beyond Traditional Precious Metals, *Chem. Asian J*. 16 (2021) 2817–2829. DOI: 10.1002/asia.202100784

[9]. V. Chopra, A.R. Kadam, H.C. Swart, S.J. Dhoble, Introduction to luminescence and radiation dosimetry techniques, *Radiat. Dosim. Phosphors* (2022) 1–27. DOI: 10.1016/B978-0-323-85471-9.00010-5

[10]. H. Zhang, H. Zhang, Special Issue: Rare earth luminescent materials, *Light Sci. Appl.* 11 (2022) 260. DOI: 10.1038/s41377-022-00956-9

[11]. J. Bauri, R.B. Choudhary, G. Mandal, Recent advances in efficient emissive materials-based OLED applications: a review, *J. Mater. Sci.* 56 (2021) 18837–18866. DOI: 10.1007/s10853-021-06503-y

[12]. J. Yang, M. Fang, Z. Li, Organic luminescent materials: The concentration on aggregates from aggregation-induced emission, *Aggregate* 1 (2020) 6–18. DOI: 10.1002/agt2.2

[13]. M.S. Seehra, A.D. Bristow, Introductory Chapter: Overview of the Properties and Applications of Noble and Precious Metals. In Noble and Precious Metals - Properties, Nanoscale Effects and Applications. InTech, 2018. DOI: 10.5772/intechopen.75503

[14]. C. Hagelüken, Markets for the Catalyst Metals Platinum, Palladium and Rhodium, *Metall* 60 (2006) 31–42. https://www.researchgate.net/publication/270686728_Markets_for_the_Catalyst_Metals_Platinum_Palladium_and_Rhodium

[15]. G. Gong, S. Xie, Y. Song, H. Tan, J. Xu, et al., Synthesis of Lanthanide-Ion-Doped NaYF4 RGB Up-Conversion Nanoparticles for Anti-Counterfeiting Application, *J. Nanosci. Nanotechnol.* 18 (2018) 8207–8215. DOI: 10.1166/jnn.2018.15801

[16]. Liwen Zheng, Yuxin Yang, Hao Wu, Huajun Wu, Guo-Hui Pan, et al., Toward Controllable Self-Reduction of Mn4+ to Mn2+ by Lanthanide Ions for Luminescence Based Colorimetric Sensing of Temperature, *Adv. Opt. Mater.* 13 (2024) 2402020. DOI: 10.1002/adom.202402020

[17]. Y. Zhang, C. Fowler, J. Liang, B. Azhar, M.Y. Shalaginov et al., Electrically reconfigurable non-volatile metasurface using low-loss optical phase-change material, *Nat. Nanotechnol.* 16 (2021) 661–666. DOI: 10.1038/s41565-021-00881-9

[18]. H. Shim, F. Monticone, O.D. Miller, Fundamental Limits to the Refractive Index of Transparent Optical Materials, *Adv. Mater.* 33 (2021) 2103946. DOI: 10.1002/adma.202103946

[19]. T.D. Creason, A. Yangui, R. Roccanova, A. Strom, M.-H. Du, B. Saparov, Rb_2CuX_3 (X = Cl, Br): 1D All-Inorganic Copper Halides with Ultrabright Blue Emission and Up-Conversion Photoluminescence, *Adv. Opt. Mater.* 8 (2020) 1901338. DOI: 10.1002/adom.201901338

[20]. J. Choi, C. Schwarz, Advances in femtosecond laser processing of optical material for device applications, *Int. J. Appl. Glass Sci.* 11 (2020) 480–490. DOI: 10.1111/ijag.14979

[21]. Y.-L. Yang, X.-C. Yang, J.-Y. Yuan, T. Li, Y.-T. Fan, et al., Time-Resolved Bright Red to Cyan Color Tunable Mechanoluminescence from CaZnOS:Bi3+, Mn2+ for Anti-Counterfeiting Device and Stress Sensor, *Adv. Opt. Mater*. 9 (2021) 2100668. DOI: 10.1002/adom.202100668

[22]. C. Cai, J. Wang, Femtosecond Laser-Fabricated Photonic Chips for Optical Communications: A Review, *Micromachines* 13 (2022) 630. DOI: 10.3390/mi13040630

[23]. M.K. Hossain, G.A. Raihan, M.A. Akbar, M.H.K. Rubel, M.H. Ahmed, et al., Current Applications and Future Potential of Rare Earth Oxides in Sustainable Nuclear, Radiation, and Energy Devices: A Review, *ACS Appl. Electron. Mater*. 4 (2022) 3327–3353. DOI: 10.1021/acsaelm.2c00069

[24]. S. Bo, J. Hu, Q. Wang, X. Liu, Z. Zhen, Near-infrared luminescence properties of erbium complexes with the substituted phthalocyaninato ligands, *Photochem. Photobiol. Sci.* 7 (2008) 474–479. DOI: 10.1039/b715809b

[25]. R. Van Deun, P. Nockemann, C. Görller-Walrand, K. Binnemans, Strong erbium luminescence in the near-infrared telecommunication window, *Chem. Phys. Lett.* 397 (2004) 447–450. DOI: 10.1016/j.cplett.2004.09.011

[26]. L. Plasseraud, Glycerol as Ligand in Metal Complexes-A Structural Review, *Crystals* 14 (2024) 217. DOI: 10.3390/cryst14030217

[27]. I. Anugwom, P. Mäki-Arvela, P. Virtanen, P. Damlin, R. Sjöholm, J.-P. Mikkola, Switchable Ionic Liquids (SILs) Based on Glycerol and Acid Gases, *RSC Adv.* 1 (2011) 452–457. DOI: 10.1039/c1ra00154j

[28]. L.G. Nersisyan, H.R. Petrosyan, A Facile Synthesis and Investigation of $Na_8[ZrErNd(MoO_4)_9]$ Complex, *Eurasian Chem.-Technol. J.* 25 (2023) 115–120. DOI: 10.18321/ectj1501

[29]. L. Nersisyan, R. Harutyunyan, A. Martiryan, H. Petrosyan, Luminescent Properties of a Solid-Phase Composite Based on Zirconium, Rare Earth Elements (Er, Nd) and Molybdenum, *Eurasian Chem.-Technol. J.* 27 (2025) 229–234. DOI: 10.18321/ectj1670

[30]. L.G. Nersisyan, R.S. Arutyunyan, H.R. Petrosyan, Study of Reactions in the Na_2MoO_4-$ZrOCl_2$-$ErCl_3$-H_2O System, *Theor. Found. Chem. Eng*. 57 (2023) 1083-1087. DOI: 10.1134/S0040579523310068

[31]. K. Nakamoto, Infrared and Raman Spectra of Inorganic and Coordination Compounds. In

Handbook of Vibrational Spectroscopy (eds J.M. Chalmers and P.R. Griffiths), USA, 2006, p. 432. DOI: 10.1002/0470027320.s4104

[32]. V.Y. Mena-Cervantes, R. Hernández-Altamirano, A. Tiscareño-Ferrer, Development of a green one-step neutralization process for valorization of crude glycerol obtained from biodiesel, *Environ. Sci. Pollut. Res.* 27 (2020) 28500–28509. DOI: 10.1007/s11356-019-07287-0

[33]. N. Chanthima, J. Kaewkhao, Properties of erbium luminescence in barium borophosphate glasses, *Mater. Today Proc.* 4 (2017) 6099–6104. DOI: 10.1016/j.matpr.2017.06.100

[34]. O.L. Malta, L.D. Carlos, Intensities of 4f–4f transitions in glass materials, *Quím. Nova* 26 (2003) 889–895. DOI: 10.1590/S0100-40422003000600018

[35]. J.-C.G. Bünzli, Lanthanide Luminescence for Biomedical Analyses and Imaging, *Chem. Rev*. 110 (2010) 2729–2755. DOI: 10.1021/cr900362e